

The Runaway Binary LP 400-22 is Leaving the Galaxy

Mukremin Kilic^{1*}, A. Gianninas¹, Warren R. Brown², Hugh C. Harris³, Conard C. Dahn³,
M. A. Agüeros⁴, Craig O. Heinke⁵, S. J. Kenyon², J. A. Panei⁶, Fernando Camilo^{4,7}

¹*Homer L. Dodge Department of Physics and Astronomy, University of Oklahoma, 440 W. Brooks St., Norman, OK, 73019, USA*

²*Smithsonian Astrophysical Observatory, 60 Garden St, Cambridge, MA 02138, USA*

³*US Naval Observatory, Flagstaff Station, 10391 West Naval Observatory Road, Flagstaff, AZ 86001, USA*

⁴*Columbia University, Department of Astronomy, 550 West 120th Street, New York, NY 10027, USA*

⁵*Department of Physics, CCIS 4-183, University of Alberta, Edmonton, AB, T6G 2E1, Canada*

⁶*Instituto de Astrofísica La Plata, IALP, CONICET-UNLP, Argentina*

⁷*Arecibo Observatory, HC3 Box 53995, Arecibo, PR 00612, USA*

15 July 2013

ABSTRACT

We present optical spectroscopy, astrometry, radio, and X-ray observations of the runaway binary LP 400-22. We refine the orbital parameters of the system based on our new radial velocity observations. Our parallax data indicate that LP 400-22 is significantly more distant (3σ lower limit of 840 pc) than initially predicted. LP 400-22 has a tangential velocity in excess of 830 km s^{-1} ; it is unbound to the Galaxy. Our radio and X-ray observations fail to detect a recycled millisecond pulsar companion, indicating that LP 400-22 is a double white dwarf (WD) system. This essentially rules out a supernova runaway ejection mechanism. Based on its orbit, a Galactic center origin is also unlikely. However, its orbit intersects the locations of several globular clusters; dynamical interactions between LP 400-22 and other binary stars or a central black hole in a dense cluster could explain the origin of this unusual binary.

Key words: binaries: close — white dwarfs — stars: individual (LP 400-22, WD 2234+222) — Galaxy: kinematics and dynamics — Galaxy: stellar content

1 INTRODUCTION

Dynamical processes involving n-body interactions in dense star clusters, supernova explosions in tight binary systems, or interactions with the black hole at the Galactic center can eject stars from their birthplace at high velocities. In the first scenario, most of the runaway stars ejected from clusters through three-, four-, or n-body interactions (Poveda et al. 1967) are expected to be single stars. However, a small fraction should be tight binaries ejected through close encounters (Gies & Bolton 1986). Binary-binary encounters may disrupt one or both systems, but in 10% of the cases, two binaries are ejected (Mikkola 1983). In the supernova ejection scenario (Blaauw 1961), all runaway binary systems contain the remnant of a supernova explosion, a neutron star or a black hole. However, in the majority of the cases, these companions cannot be detected due to selection effects, e.g. small radial velocity variations due to the low-mass of a neutron star compared to the runaway OB stars and the short lifetimes of radio pulsar companions (Portegies Zwart 2000).

Hypervelocity stars (HVSs, Brown et al. 2005, 2007;

Edelmann et al. 2005) with velocities even higher than the runaway stars, are likely ejected from the Galactic center (Hills 1988; Brown et al. 2012). So far, there are no binary HVSs known. However, several HVSs have main-sequence lifetimes significantly shorter than their travel time from the Galactic center. Perets (2009) suggests that such stars may be the result of a merger of a HVS binary system that rejuvenates itself after its ejection from the Galactic center. HE 0437–5439 (Edelmann et al. 2005; Brown et al. 2010) and US 708 (Hirsch et al. 2005) are two such systems, where the progenitor HVS binaries might have been ejected due to triple disruptions and other dynamical interactions with stars or black holes.

Lu et al. (2007) and Sesana et al. (2009) propose that the discovery of HVS binary stars would indicate the existence of a binary black hole at the Galactic center. In their model, HVS binaries with velocities $\sim 1,000 \text{ km s}^{-1}$ can be ejected from the Galactic center due to interactions with a binary black hole. Even though tidal disruption of a hierarchical triple star system by a single black hole may lead to a HVS binary, they find the ejection rate from this mechanism is negligible (although see the discussion in Perets 2009).

In this paper we revisit the unusual runaway binary

* kilic@ou.edu

LP 400-22 (WD 2234+222 at $l = 86.5^\circ$ and $b = -30.7^\circ$). Kawka et al. (2006) identified LP 400-22 as a fast moving, extremely low-mass (ELM, $0.17 M_\odot$) WD at a distance of 430 ± 45 pc. Kilic et al. (2009) and Vennes et al. (2009) obtained follow-up radial velocity observations, which demonstrated that LP 400-22 is a double degenerate binary system with an orbital period of ≈ 1 day. Based on the available astrometric data, Kilic et al. (2009) estimated that the probability of a Galactic center origin is 0.1% and concluded that LP 400-22 is most likely a halo star with an unusual orbit. Here we present additional radial velocity, astrometry, X-ray, and radio observations of LP 400-22 and revisit its origin. Our observations are discussed in Section 2, whereas the revised binary parameters and its Galactic orbit are discussed in Sections 3 and 4, respectively.

2 OBSERVATIONS

2.1 Optical Spectroscopy

We used the 6.5m MMT equipped with the Blue Channel Spectrograph to obtain additional optical spectroscopy of LP 400-22 over several nights in September 2009 and November 2010. Our observing and reduction procedures are similar to those of Kilic et al. (2009). The only difference is that most of the new spectra were obtained using a $1.25''$ slit, instead of the $1''$ slit used in our earlier work.

In addition to measuring radial velocities, we use our MMT data to revise the atmospheric parameters of the visible ELM WD in the system. Figure 1 shows the fits to the composite spectrum using the pure hydrogen atmosphere models from Tremblay & Bergeron (2009). The best fit temperature and gravity with the formal errors are $T_{\text{eff}} = 11320 \pm 40$ K and $\log g = 6.58 \pm 0.01$. The best-fit spectroscopic distance estimate is 350 pc. The temperature estimate is consistent with the previous analysis (Kawka et al. 2006; Kilic et al. 2009; Vennes et al. 2009). However, the gravity estimate is 0.16-0.28 dex higher. The improved Stark broadening profiles of the Tremblay & Bergeron (2009) models lead to an increase of ~ 0.1 dex in surface gravity for average mass WDs. We perform a similar analysis of the LP 400-22 spectrum using both old and the new models and find that the new models increase the best-fit $\log g$ estimate by 0.14 dex. Hence, the difference between the previous surface gravity measurements and ours is mostly due to the improved Stark broadening profiles in the new models.

2.2 Astrometry

Astrometric observations of LP 400-22 spanning five seasons were obtained as part of the USNO parallax program. Data acquisition and reduction procedures are described in Dahn et al. (2002). Figure 2 presents the observed parallactic motion for LP 400-22. Using 159 frames taken on 92 nights and 20 reference stars, we measure a relative proper motion of $\mu = 208.5 \pm 0.2$ mas yr $^{-1}$ at position angle $74.07^\circ \pm 0.15^\circ$, and a relative parallax of -0.42 ± 0.30 mas. Using the colors and magnitudes of the reference-frame stars, we estimate the absolute parallax to be 0.26 ± 0.31 mas. Given the relatively small parallax and its large error, we cannot constrain the actual distance to LP 400-22, but

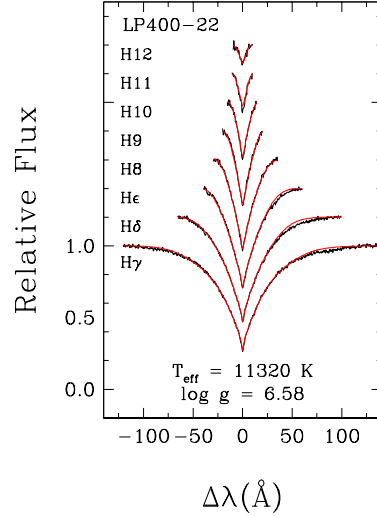


Figure 1. Spectral fits (red lines) to the MMT spectrum (black lines) of LP 400-22.

we can still use the 3σ lower limit of our parallax measurement to constrain the physical properties of the system. The nominal distance of 3.8 kpc would correspond to a tangential velocity of 3800 km s^{-1} , which is extremely unlikely. The 2σ and 3σ lower limits on the distance are 1130 and 840 pc, respectively. Our proper motion and distance measurements imply a 3σ lower limit on tangential velocity of 830 km s^{-1} , higher than the escape velocity from the Galaxy.

2.3 Radio

We observed LP 400-22 on 2008 Mar 28 for 22.5 min with the Berkeley-Caltech Pulsar Machine (BCPM Backer et al. 1997) on the Green Bank Telescope. At the central observing frequency of 820 MHz, the BCPM provided 48 MHz of bandwidth split into 96 spectral channels; for each channel we recorded total power samples every $72 \mu\text{s}$. The data reduction was similar to that described in Agüeros et al. (2009b): we used the standard search techniques implemented in the PRESTO software package (Ransom 2001). The dispersion measure range for the search was $0 - 115 \text{ cm}^{-3} \text{ pc}$.

We note that while orbital motions can affect the apparent spin period of a pulsar (i.e., if the integration time is a significant fraction of the binary orbital period), here the integration time is only about 1% of the orbital period, so that the assumption of constant apparent acceleration built into PRESTO should hold. No convincing pulsar signal is detected in our data.

2.4 X-ray

We obtained observations of LP 400-22 with XMM (ObsID 0553440201, on 2008 Nov 20) and Chandra (ObsID 9962, on 2009 July 28). We analyzed the pre-processed (PPS or event2) datasets using SAS v. 11.0 and CIAO v. 4.3. We checked all data for background flares; finding none, we used the whole datasets (livetimes of 1028 s, 4438 s, 6520 s, and 6520 s for Chandra ACIS, XMM pn, MOS1, and MOS2 respectively). We filtered the XMM datasets following stan-

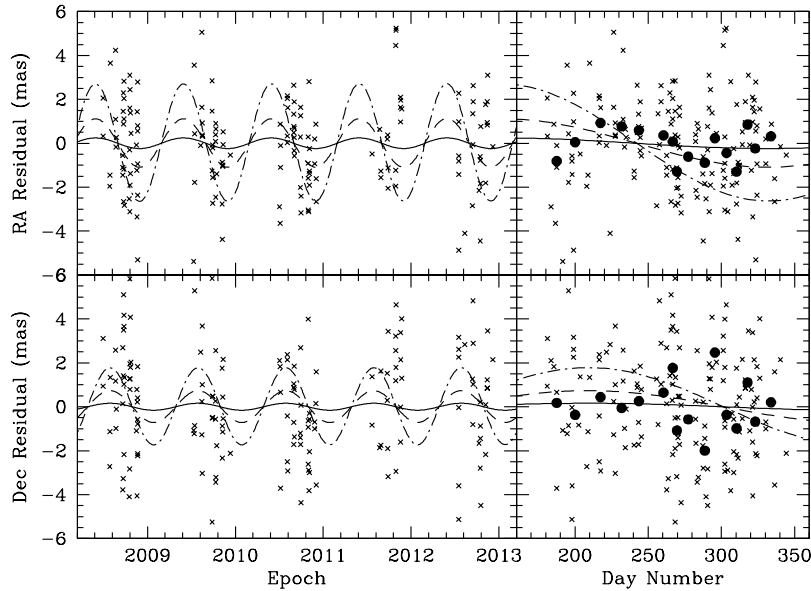


Figure 2. The observed parallactic motion in RA (top panel) and Dec (bottom panel), after fitting the astrometry for parallax and proper motion and subtracting the proper motion. The data have the correction to absolute parallax of 0.68 mas added to the observed residuals, as if the reference stars were at infinite distance. The solid curve shows the best fit parallax, the dashed line shows the 3-sigma upper limit to the parallax, and the dot-dash curve shows the parallax for the spectroscopic distance of 347 pc from Fig. 1. Right panels show the same parallax data folded on a 1 year period, with 10-point-means added (filled circles).

dard procedures¹; PATTERN ≤ 12 and standard FLAG values for the MOS and pn detectors. We created images for each detector in the energy range of 0.5 to 2 keV.

We calculate the minimum flux expected, should the companion to LP 400-22 be a (recycled) neutron star, with an X-ray luminosity (L_X (0.3-2 keV) = 1.5×10^{30} ergs cm⁻² s⁻¹) and spectrum (134 eV blackbody) equal to that of the faintest millisecond pulsar in 47 Tuc (Heinke et al. 2005; Bogdanov et al. 2006; see Agüeros et al. 2009a for the rationale). Assuming a distance of 1.5 kpc and $N_H = 4.5 \times 10^{20}$ cm⁻², we predict 0.75, 10, 6, and 6 counts in each detector, using the simulator PIMMS² and the exposure times and energy range above.

For the Chandra observation, we searched for emission from a 2'' circle centered on LP 400-22's position in the 0.5-2 keV band, but found zero counts. We searched for emission from 10'' circles in the XMM images, and found one event in the pn image, and one event in the combined MOS1 and MOS2 image. From XMM encircled energy calculations, we find that 60% of the encircled energy should be located within these 10'' extraction regions, so we revise our predicted counts to 6 counts in the searched region of the pn image, and 3.6 counts in this region of the combined MOS image. Combining the XMM and Chandra studied regions, we expect to see 10.4 counts, and only see two. Using Poisson statistics (Gehrels 1986), we conclude that we can rule out the hypothesis of a minimal-flux millisecond pulsar at >99.5% confidence, even at the extreme distance of 1.5

kpc. We can rule-out millisecond pulsar companions at 90% confidence level out to about 2 kpc. Clearly, LP 400-22 must be within 2 kpc of the Sun for it to have a reasonable tangential velocity of $\leq 2,000$ km s⁻¹. Therefore, we conclude that the companion must be a WD.

3 RESULTS

3.1 Orbital Parameters

We provide improved orbital parameters of the LP 400-22 binary using the radial velocity measurements from Kilic et al. (2009), Vennes et al. (2009), and our new spectroscopy data. Table 1 lists our 29 new radial velocity measurements. Figure 3 presents 53 radial velocity measurements obtained over 1500 days and the best-fit orbit with $P = 1.01014(5)$ d, $K = 119.3(8)$ km s⁻¹, and systemic velocity $\gamma = -172.0(5)$ km s⁻¹. The revised mass function is $f = 0.1778(36)$. These orbital parameters are consistent with $P = 1.01016(5)$ d and $f = 0.180(9)$ from Vennes et al. (2009) within the errors.

3.2 Physical Properties

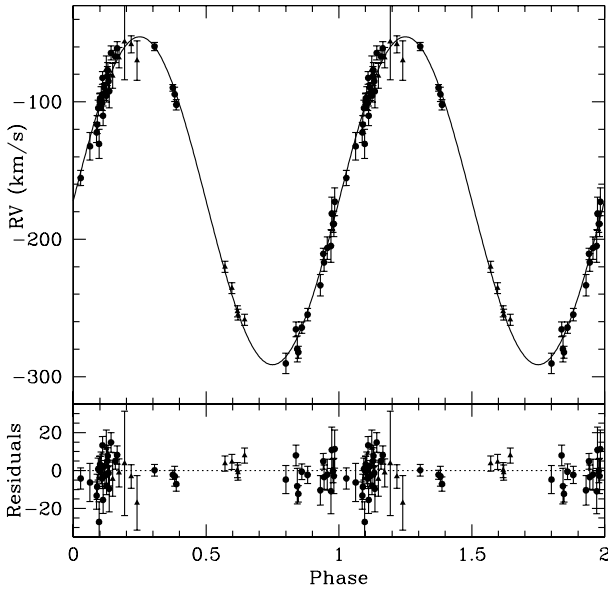
Figure 4 compares the luminosity, effective temperature, and surface gravity of the primary star in LP 400-22 to the evolutionary sequences for 0.15-0.24 M_\odot WDs from Serenelli et al. (2001) and Panei et al. (2007). The 3σ lower limit on distance indicates an absolute magnitude of $M_V = 7.6$ mag, $\log L/L_\odot = -1.05$, and $R = 0.099R_\odot$. These are consistent with the Serenelli et al. (2001) models for a 0.16 M_\odot WD with a thick hydrogen envelope. However,

¹ <http://heasarc.gsfc.nasa.gov/docs/xmm/abc/>

² <http://asc.harvard.edu/toolkit/pimms.jsp>

Table 1. New Radial Velocity Measurements for LP 400-22

HJD-2455000 (days)	v_{helio} (km s ⁻¹)
94.81508	-102.2 ± 3.8
100.61535	-77.1 ± 5.7
100.64317	-67.0 ± 4.4
100.65032	-61.1 ± 4.8
100.79241	-59.8 ± 3.0
101.59483	-100.0 ± 5.7
101.59985	-97.4 ± 8.4
101.60701	-110.2 ± 7.1
101.61413	-93.5 ± 5.5
101.62249	-81.2 ± 6.9
101.62961	-92.3 ± 12.1
101.63677	-64.5 ± 5.1
101.87234	-89.8 ± 2.4
102.59303	-122.3 ± 7.2
102.59914	-104.5 ± 5.8
102.60759	-100.5 ± 3.9
102.61494	-82.6 ± 4.6
102.62206	-89.7 ± 3.1
102.63034	-95.4 ± 4.7
102.88991	-94.6 ± 5.2
511.56650	-206.4 ± 8.2
511.58061	-204.9 ± 11.9
511.58308	-181.4 ± 12.1
511.59159	-188.9 ± 9.3
511.59425	-172.7 ± 10.1
512.68415	-132.4 ± 10.0
512.71175	-116.5 ± 6.6
512.75448	-85.1 ± 6.8
513.72902	-130.7 ± 10.6

**Figure 3.** Radial velocity measurements of LP 400-22 from Kilic et al. (2009), Vennes et al. (2009), and this work. The solid line represents the best-fit model for a circular orbit with a period of 1.01014 d and $K = 119.3$ km s⁻¹.

these models predict a surface temperature of 9600 K and $\log g = 5.6$, an order of magnitude lower in surface gravity than the best-fit model shown in Figure 1.

Clearly, there is no single model that matches all of the properties of the primary star in LP 400-22. A $0.19 M_{\odot}$ WD model can match the the best-fit temperature and surface gravity measurements, but it underpredicts the absolute magnitude, radius, and distance. Such a discrepancy between the model and parallax distance measurement for an average mass ($0.6 M_{\odot}$) DA WD could indicate the existence of spectroscopically invisible helium.

Increased pressure broadening of hydrogen lines due to the presence of helium can imitate a higher surface gravity. GD 362 is perhaps the best example of such a system, where the initial model atmosphere analysis showed that the optical spectrum can be explained by a massive ($1.2 M_{\odot}$) DA WD (Gianninas et al. 2004). However, follow-up high resolution observations (Zuckerman et al. 2007) and a parallax measurement (Kilic et al. 2008) showed that GD 362 indeed has a helium dominated atmosphere and that it is not a massive WD. Since He becomes transparent below about 11,000 K, it is possible to hide significant amounts of He in the atmosphere of LP 400-22. To investigate this possibility and to check whether a mixed H/He atmosphere solution would give results consistent with the parallax measurement, we computed model atmospheres with He/H ratios ranging from 0 to 100.

Figure 5 shows the Balmer line profiles of LP 400-22 compared to mixed atmosphere models with $T_{\text{eff}} = 9600$ K, $\log g = 5.6$ (see the above discussion), and He/H = 0, 1, 10, and 20. None of these models provide a reasonable fit to the observed spectrum of LP 400-22. This is because the addition of helium to a $\log g = 6$ atmosphere does not have the same effect as that of a $\log g = 8$ or 9 atmosphere. In addition, the spectral energy distribution analysis of Kawka et al. (2006) using ultraviolet and optical photometry is in excellent agreement with the Balmer line analysis using pure H models. Hence, a temperature as low as 9600 K can be ruled out from both spectroscopy and photometry.

Figure 6 shows the temperature, pressure, and Balmer line profiles of mixed H/He atmosphere models with He/H = 20 and $\log g = 6, 7, 8$, and 9. The pressure for the $\log g = 6$ model is two orders of magnitude smaller than it is for the $\log g = 9$ model. The results are similar for models with different He/H ratios, e.g. He/H = 50, 100. Hence, the effect of helium on the atmospheric structure and the Balmer line profiles is negligible for low surface gravity models appropriate for ELM WDs, including LP 400-22. Figures 5 and 6 demonstrate that the addition of He in our spectral models for LP 400-22 does not resolve the discrepancy between the observed properties and the evolutionary models.

An alternative explanation for the discrepancy in the spectroscopic distance estimate is an unresolved DA + DC WD system, where the DC WD companion is bright enough to contribute to the spectral continuum but not to the Balmer line profiles. We tested this scenario by fitting the observed spectrum as a composite DA + DC system. We fixed the $\log g$ of the DC component to $\log g = 7.5$ or 7.7 (0.4 or $0.5 M_{\odot}$) and allowed the other three parameters, temperature and surface gravity of the DA component and the temperature of the DC component, to vary. Our fitting algorithm achieves a good fit to the observed spectrum only

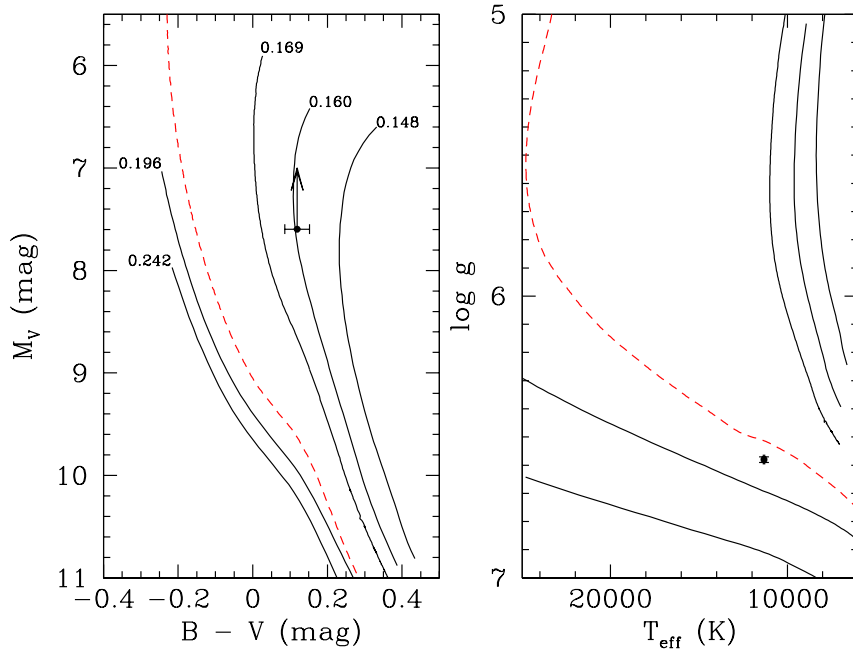


Figure 4. LP 400-22 on a color-magnitude diagram (left) and a T_{eff} vs. $\log g$ diagram. Evolutionary model sequences for $0.15\text{--}0.24 M_{\odot}$ He-core WDs (solid lines, Serenelli et al. 2001) and $0.19 M_{\odot}$ WDs (dashed lines, Panei et al. 2007) are also shown.

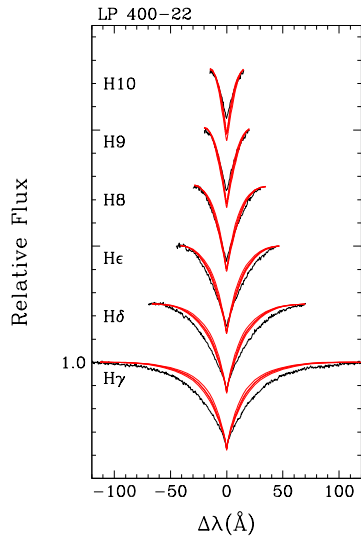


Figure 5. The MMT spectrum (black lines) of LP 400-22 compared to mixed atmosphere models with $T_{\text{eff}} = 9600$ K, $\log g = 5.6$, and $\text{He}/\text{H} = 0, 1, 10$, and 20 (from top to bottom, red lines). The Balmer line profiles for these mixed atmosphere models are essentially identical to each other due to the low surface gravity.

if the DC component is cool enough ($T_{\text{eff}} < 3500$ K) that it essentially does not contribute any light to the system. We do not find any plausible solutions involving a composite DA + DC spectrum.

Althaus et al. (2001) and Serenelli et al. (2001) predict that $M \geq 0.2 M_{\odot}$ WDs suffer from diffusion-induced hydrogen shell flashes that lead to thin hydrogen envelopes. The surface gravity and temperature measurements for LP 400-22 place it right in the transition region between the objects with and without hydrogen shell flashes (see Fig. 3).

Panei et al. (2007) argue that the lower mass limit for shell flashes is $0.17 M_{\odot}$. Below this mass limit, WDs have a thick hydrogen surface layer that provides energy through stable hydrogen burning. This extra energy source slows down the evolution of the lowest mass WDs, keeping them luminous for longer than expected. Based on the Panei et al. (2007) models, the temperature and surface gravity measurements for LP 400-22 imply a $\approx 0.19 M_{\odot}$ WD with a thin H envelope of $\log M/M_{\star} = -3.1$. On the other hand, its luminosity and colors do not match any of the Panei et al. (2007) cooling tracks; LP 400-22 may be a pre-WD.

The mass estimate for LP 400-22 ranges from $0.16 M_{\odot}$ to $0.19 M_{\odot}$. The observed parallax implies that LP 400-22 is significantly more luminous than initially predicted from the models. However, given the uncertainties in models and specifically the transition from hydrogen shell flashes to stably burning envelopes for $\approx 0.2 M_{\odot}$ WDs, it is perhaps not surprising to find discrepancies between the model expectations and the observed properties. Regardless of these issues, the observed surface gravity of the primary star in LP 400-22 shows that it is clearly a WD, and its brightness suggests that it is likely to have a thick envelope with stable hydrogen burning.

We note that the ELM WD in the eclipsing double WD binary NLTT 11748 (Steinfadt et al. 2010) looks like a cooler version of the primary star in LP 400-22. NLTT 11748 has essentially the same surface gravity as LP 400-22, but the primary WD has $T_{\text{eff}} = 8690 \pm 140$ K. NLTT 11748 was also observed as part of the USNO Parallax Program, and the distance measurement agrees with model expectations for that star (H. C. Harris 2013, private communication). Hence, the difference between the NLTT 11748 and LP 400-22 ELM WDs may be a slight difference in mass and a significant difference in the thickness of the surface hydrogen layer.

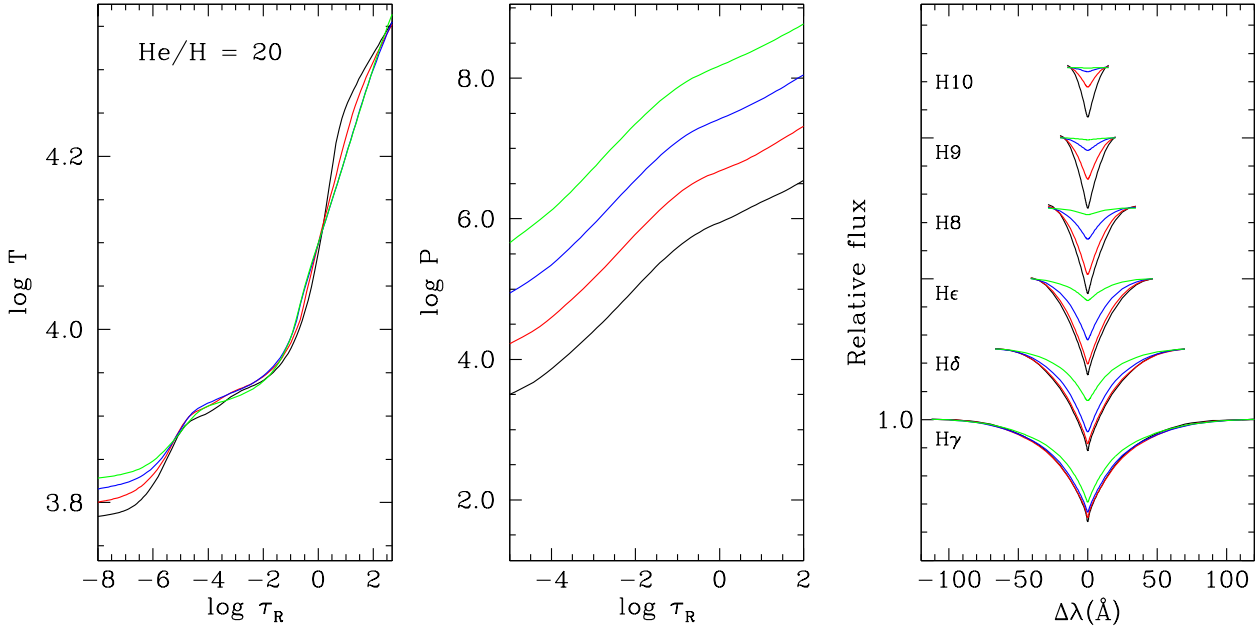


Figure 6. Temperature (left), pressure (middle), and Balmer line profiles (right) of model atmospheres with $\text{He}/\text{H} = 20$, $T_{\text{eff}} = 11,500$ K, and $\log g = 6, 7, 8$, and 9 (from bottom to top).

3.3 The Galactic Orbit

The lack of a signature of a millisecond pulsar companion in the radio and X-ray observations demonstrate that LP 400-22 is a double WD binary system containing an ELM WD and an invisible higher mass ($M \geq 0.39M_{\odot}$) WD companion at an inclination larger than 33° .

Figure 7 presents its Galactic orbit assuming a static disk-halo-bulge potential (Kenyon et al. 2008), 250 km s^{-1} solar rotation (Reid et al. 2009), the local standard of rest as defined by Schönrich et al. (2010), and $X = 8 \text{ kpc}$ and $Z = 20 \text{ pc}$ for the location of the Sun (Reed 2006). Even at the 3σ lower limit of 840 pc , LP 400-22 is unbound.

For the three trajectories shown in Figure 7, the closest pericenter passage occurs 2-9 Myr ago at distances of 0.9-3.9 kpc. Hence, a Galactic center origin is effectively ruled out for LP 400-22. The main problem is that the W component of the velocity, -140 (-220) km s^{-1} for the 3σ (2σ) lower limit on distance, is too large for a trajectory originating in the Galactic center. We note that the use of a different Galactic potential, i.e. that of Gnedin et al. (2005), does not change any of our conclusions.

4 DISCUSSION

LP 400-22 is an unbound runaway binary WD system. There are other binary runaway systems known; roughly 5% to 26% of runaway O-type stars are binary systems (Mason et al. 1998). However, LP 400-22 is unique, since it is the only runaway binary WD system currently known and it has an extremely large space velocity compared to typical runaway stars.

Unlike the neutron star companions to OB stars, a neutron star companion to LP 400-22 should be detected as

a recycled millisecond pulsar through radial velocity, radio, and X-ray observations. Our observations indicate that LP 400-22 binary has a circular orbit with no evidence of a neutron star companion. In addition, $<1\%$ of runaways are expected to receive velocity kicks in excess of 200 km s^{-1} (Portegies Zwart 2000). The observed space velocity of LP 400-22 and the non-detection of a neutron star companion indicate that the supernova ejection mechanism cannot explain the origin of the LP 400-22 binary.

Hypervelocity binary systems may form due to the tidal disruption of a hierarchical triple star by the central black hole or the interaction of a binary star with a binary black hole at the Galactic center. Lu et al. (2007) estimate that the latter formation channel can form hypervelocity binary systems with velocities up to $1,000 \text{ km s}^{-1}$. However, LP 400-22 has a Galactic orbit that is inconsistent with a Galactic center origin. Hence, the Galactic center ejection mechanism through interactions with the central black hole(s) also cannot explain the origin of the LP 400-22 binary.

An alternative birthplace where interactions with an intermediate mass black hole can take place and the number density of the stellar population is high enough for frequent close encounters is globular clusters. Multi-body interactions in a dense star cluster can in principle explain the origin of LP 400-22. Some runaway stars can be traced back to their birthplace because of their short main-sequence lifetimes and their proximity to known clusters, associations, or H II regions. In the case of LP 400-22, its WD age and total age are uncertain, and there is no way to confirm its birthplace given the uncertainties in its distance measurement. Nevertheless, an origin in a globular cluster is possible.

Figure 8 shows the Galactic orbit for LP 400-22 for the past 30 Myr along with the positions of the known globular clusters (Harris 1996). For a distance of 840 pc , 4.2 Myr ago LP 400-22 was within 170 pc of the globular cluster

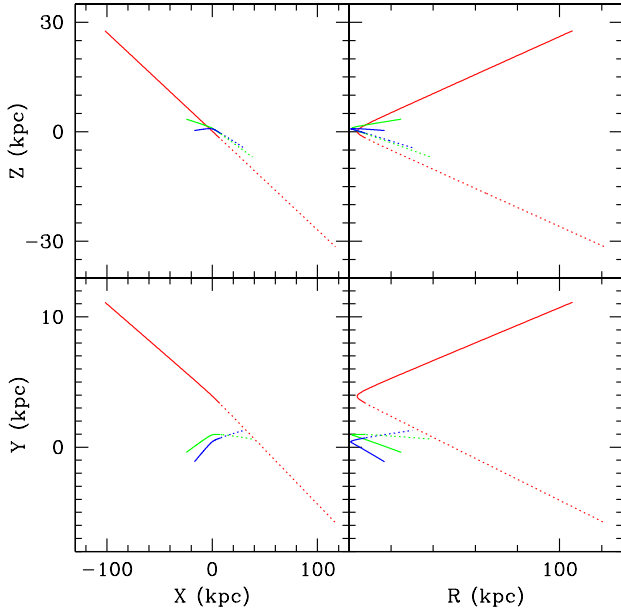


Figure 7. Galactic orbit of LP400-22 for a distance of 3800 pc (red), 1130 pc (green, 2σ lower limit), and 840 pc (blue, 3σ lower limit). The solid and dotted lines show the past and future orbits for 30 Myr.

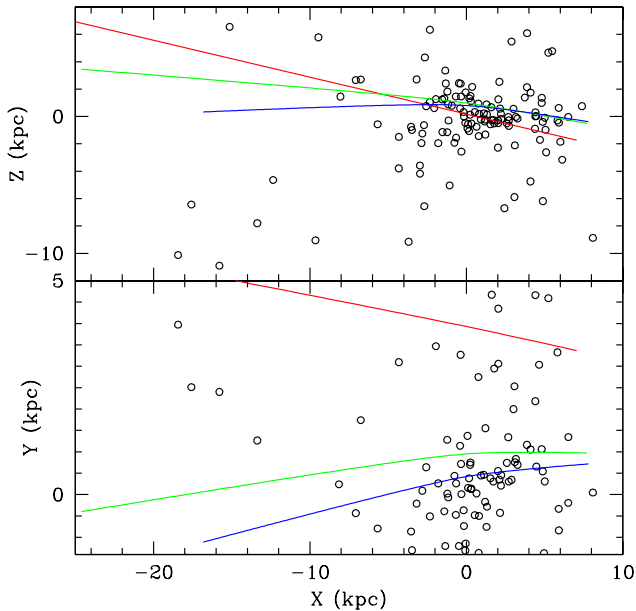


Figure 8. Galactic orbit of LP400-22 for the past 30 Myr. The symbols are the same as in Figure 7. Open circles show the positions of the known globular clusters.

2MASS-GC01. Given the uncertainties in distance, it is not possible to locate the cluster that LP 400-22 definitely came from. However, this figure demonstrates that there are several globular clusters in the vicinity of LP 400-22's trajectory that may explain its origin.

There are only a handful of hypervelocity stars with ac-

curate proper motion measurements. The problem is that many of them are located at ~ 100 kpc; space based telescopes are required to measure their proper motion. Brown et al. (2010) used the *Hubble Space Telescope* to measure the proper motion of the hypervelocity star HE 0437-5439, and demonstrated that its velocity vector points directly away from the Galactic center. Similar observations of the other known hypervelocity stars are required to directly link them to the Galactic center.

There are two cases where accurate proper motions are available and they are inconsistent with a Galactic center origin. HD 271791 is an $11 M_{\odot}$ B-type star with a velocity larger than the Galactic escape velocity. Heber et al. (2008) show that its kinematic properties rule out a Galactic center origin, and they are more consistent with the formation in the outer disk. Similarly, SDSS J013655.91+242546.0 is a $2.5 M_{\odot}$ A-type main-sequence star, likely unbound to the Galaxy and with an origin near the outer Galactic disk (Tillich et al. 2009). LP 400-22 joins this group of runaway stars for which a Galactic center origin is ruled out based on proper motion measurements.

Gualandris & Portegies Zwart (2007) and Gvaramadze et al. (2008) argue that close encounters between two hard binaries or interactions with an intermediate-mass ($\sim 10^3 M_{\odot}$) black hole in a dense environment can explain hypervelocity stars like HE 0437-5439, assuming that it originated in a star cluster in the Large Magellanic Cloud (LMC). Even though we now know that HE 0437-5439 did not originate in the LMC (Brown et al. 2010), the same arguments can be used to explain the origin of the LP 400-22 binary system in a Milky Way globular cluster. Hard binary interactions can eject single stars with velocities up to $1,400 \text{ km s}^{-1}$ (Leonard 1991). The ejection velocity can be as large as $2,300 \text{ km s}^{-1}$, if the binaries involved in the interaction consist of low-mass systems that have already gone through common-envelope evolution (Gvaramadze et al. 2008). Even though detailed dynamical simulations for the LP 400-22 binary are currently not available, it is likely that LP 400-22 formed through multi-body interactions involving hard binaries and/or an intermediate-mass black hole in a dense cluster.

5 CONCLUSIONS

We refine the orbital parameters of the intriguing runaway binary WD LP 400-22. Based on our parallax measurements, we demonstrate that this binary is unbound to the Galaxy. We estimate its Galactic orbit using a static disk-halo-bulge potential and find a Galactic center origin unlikely. No neutron star companion is detected in the radio and X-ray data, indicating that a supernova ejection mechanism is ruled out for this system. The only remaining explanation for the unusual space velocity of LP 400-22 is multi-body interactions involving hard binary systems or the disruption of a hierarchical triple system by an intermediate-mass black hole in a dense cluster. LP 400-22's trajectory intersects several known globular clusters. However, due to the relatively uncertain distance measurement, we cannot link LP 400-22 with any single globular cluster. Further follow-up parallax observations at the USNO and with the GAIA satellite will be extremely helpful in constraining the Galactic orbit for

LP 400-22. In addition, dynamical simulations specifically designed to study the LP 400-22 binary WD system will be useful for understanding its origin in a dense cluster and its implications for the existence of intermediate-mass black holes in globular clusters.

ACKNOWLEDGEMENTS

We thank P. Bergeron for useful discussions on mixed model atmospheres and S. Vennes for a constructive referee report. MK is thankful to the University of Oklahoma Research Council and the College of Arts and Sciences for a Junior Faculty Fellowship. CH is supported by an NSERC Discovery Grant, and by an Alberta Ingenuity New Faculty Award. Part of the observations reported here were obtained at the MMT Observatory, a joint facility of the Smithsonian Institution and the University of Arizona. The Robert C. Byrd Green Bank Telescope is operated by the National Radio Astronomy Observatory, which is a facility of the US National Science Foundation operated under cooperative agreement by Associated Universities, Inc.

Facilities: MMT, CXO, XMM, GBT

REFERENCES

- Agüeros, M. A., Camilo, F., Silvestri, N. M., et al. 2009a, *ApJ*, 697, 283
- Agüeros, M. A., Heinke, C., Camilo, F., et al. 2009b, *ApJ*, 700, L123
- Althaus, L. G., Serenelli, A. M., & Benvenuto, O. G. 2001, *MNRAS*, 323, 471
- Backer, D. C., Dexter, M. R., Zepka, A., et al. 1997, *PASP*, 109, 61
- Blaauw, A. 1961, *Bull. Astron. Inst. Netherlands*, 15, 265
- Bogdanov, S., Grindlay, J. E., & Rybicki, G. B. 2006, *ApJ*, 648, L55
- Brown, W. R., Geller, M. J., Kenyon, S. J., & Kurtz, M. J. 2005, *ApJ*, 622, L33
- Brown, W. R., Geller, M. J., Kenyon, S. J., Kurtz, M. J., & Bromley, B. C. 2007, *ApJ*, 671, 1708
- Brown, W. R., Anderson, J., Gnedin, O. Y., et al. 2010, *ApJ*, 719, L23
- Brown, W. R., Cohen, J. G., Geller, M. J., & Kenyon, S. J. 2012, *ApJ*, 754, L2
- Dahn, C. C., Harris, H. C., Vrba, F. J., et al. 2002, *AJ*, 124, 1170
- Edelmann, H., Napiwotzki, R., Heber, U., Christlieb, N., & Reimers, D. 2005, *ApJ*, 634, L181
- Gehrels, N. 1986, *ApJ*, 303, 336
- Gianninas, A., Dufour, P., & Bergeron, P. 2004, *ApJ*, 617, L57
- Gies, D. R., & Bolton, C. T. 1986, *ApJS*, 61, 419
- Gnedin, O. Y., Gould, A., Miralda-Escudé, J., & Zentner, A. R. 2005, *ApJ*, 634, 344
- Gualandris, A., & Portegies Zwart, S. 2007, *MNRAS*, 376, L29
- Gvaramadzé, V. V., Gualandris, A., & Portegies Zwart, S. 2008, *MNRAS*, 385, 929
- Harris, W.E. 1996, *AJ*, 112, 1487
- Heber, U., Edelmann, H., Napiwotzki, R., Altmann, M., & Scholz, R.-D. 2008, *A&A*, 483, L21
- Heinke, C. O., Grindlay, J. E., Edmonds, P. D., et al. 2005, *ApJ*, 625, 796
- Hills, J. G. 1988, *Nature*, 331, 687
- Hirsch, H. A., Heber, U., O'Toole, S. J., & Bresolin, F. 2005, *A&A*, 444, L61
- Kawka, A., Vennes, S., Oswalt, T. D., Smith, J. A., & Silvestri, N. M. 2006, *ApJ*, 643, L123
- Kenyon, S. J., Bromley, B. C., Geller, M. J., & Brown, W. R. 2008, *ApJ*, 680, 312
- Kilic, M., Thorstensen, J. R., & Koester, D. 2008, *ApJ*, 689, L45
- Kilic, M., Brown, W. R., Allende Prieto, C., Swift, B., Kenyon, S. J., Liebert, J., & Agüeros, M. A. 2009, *ApJ*, 695, L92
- Leonard, P. J. T. 1991, *AJ*, 101, 562
- Lu, Y., Yu, Q., & Lin, D. N. C. 2007, *ApJ*, 666, L89
- Mason, B. D., Gies, D. R., Hartkopf, W. I., et al. 1998, *AJ*, 115, 821
- Mikkola, S. 1983, *MNRAS*, 203, 1107
- Panei, J. A., Althaus, L. G., Chen, X., & Han, Z. 2007, *MNRAS*, 382, 779
- Perets, H. B. 2009, *ApJ*, 698, 1330
- Portegies Zwart, S. F. 2000, *ApJ*, 544, 437
- Poveda, A., Ruiz, J., & Allen, C. 1967, *Boletín de los Observatorios Tonantzintla y Tacubaya*, 4, 86
- Ransom, S. M. 2001, *Bulletin of the American Astronomical Society*, 33, #119.03
- Reed, B. C. 2006, *Journal of the Royal Astronomical Society of Canada*, 100, 146
- Reid, M. J., Menten, K. M., Zheng, X. W., et al. 2009, *ApJ*, 700, 137
- Schönrich, R., Binney, J., & Dehnen, W. 2010, *MNRAS*, 403, 1829
- Serenelli, A. M., Althaus, L. G., Rohrmann, R. D., & Benvenuto, O. G. 2001, *MNRAS*, 325, 607
- Sesana, A., Madau, P., & Haardt, F. 2009, *MNRAS*, 392, L31
- Steinfadt, J. D. R., Kaplan, D. L., Shporer, A., Bildsten, L., & Howell, S. B. 2010, *ApJ*, 716, L146
- Tillich, A., Przybilla, N., Scholz, R.-D., & Heber, U. 2009, *A&A*, 507, L37
- Tremblay, P.-E., & Bergeron, P. 2009, *ApJ*, 696, 1755
- Vennes, S., Kawka, A., Vaccaro, T. R., & Silvestri, N. M. 2009, *A&A*, 507, 1613
- Zuckerman, B., Koester, D., Melis, C., Hansen, B. M., & Jura, M. 2007, *ApJ*, 671, 872